Determination of the rotational population of H_2 and D_2 including high-N states in low temperature plasmas via the Fulcher-α transition

S. Briefi[a,*], D. Rauner[a,b], U. Fantz[a,b]

[a] *AG Experimentelle Plasmaphysik, Universität Augsburg, 86135 Augsburg, Germany*
[b] *Max-Planck-Institut für Plasmaphysik, Boltzmannstr. 2, 85748 Garching, Germany*

Abstract

Vibrational and rotational excitation of the hydrogen molecule can significantly effect molecular reaction rates in low pressure low temperature plasmas, for example for the creation of H^-/D^- ions via the dissociative attachment process. In general, the rotational population in these discharges is known to be non-thermal with an overpopulation of states with high rotational quantum number N. In contrast to a sophisticated direct measurement of the rotational distribution in the $X\ ^1\Sigma_g^+, v = 0$ state, it is demonstrated that the determination can also be carried out up to high-N levels rather easily via optical emission spectroscopy utilizing the Fulcher-α transition of H_2 and D_2. The measured rotational populations can be described with a two-temperature distribution where the cold part reflects the population according to the gas temperature of the discharge. This has been verified by using the emission of the second positive system of nitrogen as independent gas temperature diagnostic. The hot part where the rotational temperature reaches several thousand Kelvin arises most probably from recombinative desorption of hydrogen at the discharge vessel wall where parts of the binding energy are converted into rotational excitation. Neglecting the hot population - what is often done when using the Fulcher-α transition as gas temperature diagnostic - can lead to a strong overestimation of T_{gas}. No fundamental differences in the rotational distributions between hydrogen and deuterium have been found, only the hot rotational temperature is smaller for D_2 indicating an isotope-dependency of the recombinative desorption process.

Keywords: Rotational population, Diatomic molecules, Gas temperature determination, Molecular emission

*Corresponding author
Email address: stefan.briefi@physik.uni-augsburg.de (S. Briefi)

1. Introduction

For hydrogen discharges, it is well known that rovibrational excitation of the H_2 molecule can have a significant impact on several molecular reaction rates. The correct consideration of these processes plays a key role for a detailed understanding of these plasmas, for example concerning H^- or D^- densities in negative hydrogen ion sources [1]. In the plasma volume, H^-/D^- ions are formed by dissociative attachment of electrons to the hydrogen molecule. For H_2 (D_2), the reaction rate increases by five (seven) orders of magnitude if the molecule is vibrationally excited to a state with the vibrational quantum number $v = 5$ ($v = 6$) [2]. Rotational excitation has an analogous effect as the rate is only dependent on the total internal energy of the molecule and not on the exact fraction of the energy in the particular rotational or vibrational modes [3].

In low pressure hydrogen discharges the rotational levels in the electronic ground state are known to be populated in a non-thermal way: Rotational states with low rotational quantum number follow a Boltzmann distribution according to the gas temperature of the discharge whereas those levels with high quantum number are overpopulated by several orders of magnitude (see for example [4, 5, 6, 7, 8, 9] for hydrogen and [10, 11, 12] for deuterium). Different processes that could contribute to the overpopulation in general have been evaluated in detail in [9]. It turned out that the reaction behind the overpopulation - which is present in all vibrational states - is most probably recombinative desorption of hydrogen at the wall of the discharge vessel where parts of the energy from the exothermic reaction are converted into rotational excitation.

Despite the high overpopulation of the rotational states and its potentially considerable influence on the molecular reaction rates, direct measurements of rovibrational populations in the electronic ground state are rarely carried out. This arises from the fact that rather complex and expensive diagnostic methods such as coherent anti-Stokes Raman scattering (CARS) spectroscopy [7, 10, 11], resonantly enhanced multi-photon ionization (REMPI) [4], VUV laser absorption spectroscopy [5, 6] or laser induced fluorescence (where the laser radiation is generated via stimulated anti-Stokes Raman scattering) [8, 9] are required.

In contrast, the determination of the rotational population of the $v = 0$ level in the electronic ground state presented in this paper is based on optical emission spectroscopy measurements of the Fulcher-α transition ($d\ ^3\Pi_u \rightarrow a\ ^3\Sigma_g^+$). This emission band is located in the visible spectral range and is routinely evaluated for obtaining the gas temperature of a discharge from the rotational population of the $d\ ^3\Pi_u$ state since Lavrov's pioneering work [13, 14, 15]. Typically, these measurements are restricted to levels with rather low rotational quantum numbers. In this paper, the evaluation of the Fulcher-α transition is extended to the first twelve (for D_2 13) rotational levels what allows an easy assessment of the non-thermal part of the rotational population. It should be noted that such a distribution may also alter the direct correlation between the rotational temperature and the gas temperature T_{gas} in general [16]. In order to check if T_{gas} corresponds to the rotational temperature of the low lying states, measurements with varying nitrogen admixtures to hydrogen and deuterium plasmas

have been carried out. From the evaluation of the emission arising from the second positive system of nitrogen, a reliable value for the gas temperature can be obtained [16].

2. The Fulcher-α transition of molecular hydrogen

The Fulcher-α spectrum which arises from the transition from the $d\ ^3\Pi_u$ into the $a\ ^3\Sigma_g^+$ state is located between 520 and 770 nm but the most intense part lies at $590 - 650$ nm. It is typically the most intense emission of the hydrogen molecule in low pressure plasmas why it is often utilized for diagnostics concerning the rotational or vibrational population. Details of the Fulcher-α transition and the properties of the involved electronic states have been described extensively multiple times (see for example [17, 14]), therefore only the most important facts are given in the following. The upper electronic state is split into the $d\ ^3\Pi_u^+$ and $d\ ^3\Pi_u^-$ states because of λ-doubling. Due to optical selection rules, the Q branch of the Fulcher-α transition originates only from the $d\ ^3\Pi_u^-$ state whereas the P and R branch originate from the $d\ ^3\Pi_u^+$ state. The latter two branches are not considered in the present investigation as the $d\ ^3\Pi_u^+$ state is strongly perturbed by other electronic states [18, 19] leading to anomalies in the intensities of the emitted lines [20].

In the upper $d\ ^3\Pi_u^-$ state, the dissociation limit of H_2 to H(1s) and H(2s) is located between the energy levels of the vibrational states $v' = 3$ and $v' = 4$ [21, 22]. Predissociation leads to non-radiative decay of the states and therefore the Fulcher-α emission gets considerably weaker for transitions involving states with $v' \geq 4$ [23]. For deuterium the limit is between the states $v' = 4$ and $v' = 5$ and transitions from $v' \geq 5$ are much weaker [18]. Therefore, the evaluations carried out in this paper are restricted to the vibrational states $v' = 0, 1, 2$ & 3 both for deuterium and hydrogen. In addition, only the diagonal vibrational transitions with $v' = v''$ are considered as they represent the most intense emission bands within the electronic transition. Figure 1 shows an exemplary Fulcher-α emission spectrum of hydrogen where the position of the Q lines from the first four diagonal vibrational transitions are depicted. The line positions have been taken from [24]. Figure 2 shows the same spectrum but for deuterium, the line positions have been taken from [25]. Due to the larger mass of the deuterium molecule, the wavelength separation of the individual emission lines is smaller in comparison to hydrogen. A zoom into the region just above 600 nm is depicted in Figure 3 in order to demonstrate that the individual lines of the Fulcher-α transition are well resolved both for H_2 and D_2 with the utilized spectroscopic setup (see section 4 for details on the setup). This is important for the detailed evaluation described in this paper.

In low pressure low temperature discharges, the $d\ ^3\Pi_u^-$ state is predominantly populated by electron impact excitation out of the ground state $X\ ^1\Sigma_g^+$ [14, 17]. It has been shown that the selection rule $\Delta N = 0$ holds for this process (for denoting the rotational levels the quantum number N should be used instead of J as the electronic states belong to Hund's coupling case b) [17] which means that the rotational distribution is preserved during the excitation process. In the

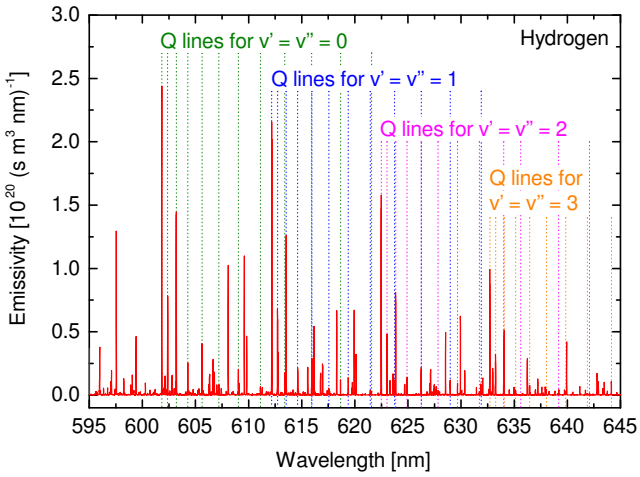

Figure 1: Example spectra of the Fulcher-α emission of hydrogen recorded in an ICP operated at 1 Pa with an RF power of 600 W. The Q lines of the first four diagonal vibrational transitions ($v' = v''$) considered in the evaluations are depicted.

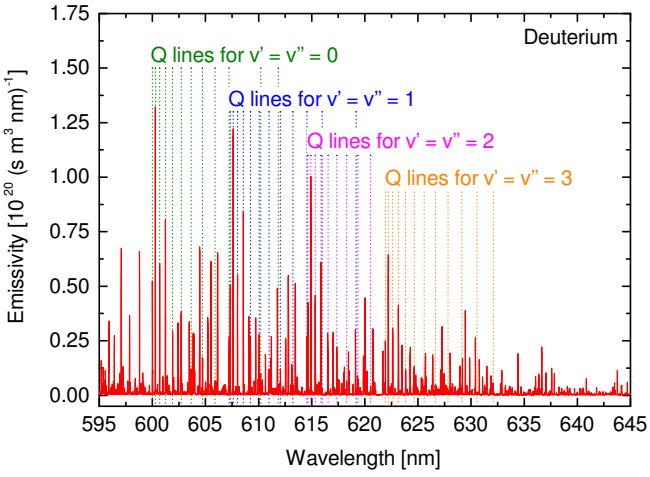

Figure 2: Example spectra of the Fulcher-α emission of deuterium recorded in an ICP operated at 1 Pa with an RF power of 600 W. The Q lines of the first four diagonal vibrational transitions ($v' = v''$) considered in the evaluations are depicted.

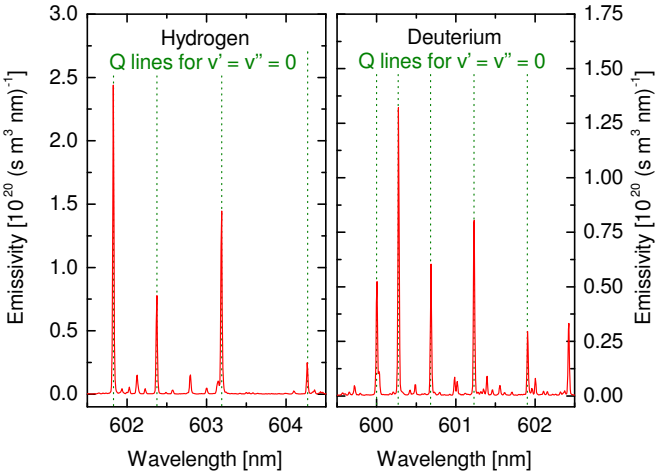

Figure 3: Zoom into the spectra shown in Figure 1 and 2 respectively.

excited $d\ ^3\Pi_u^-$ state a redistribution of the rotational population, for example by inelastic heavy particle collisions, does not occur as the lifetime of the considered vibrational levels is rather short being around 40 ns both for H_2 and D_2 [26]. Furthermore, the contribution of cascades from higher lying electronic states to the population of the $d\ ^3\Pi_u$ state has been estimated to 10% in a discharge with high electron temperatures and densities of $T_e = 100 - 200$ eV and $n_e \approx 10^{18}$ m^{-3} [17]. In typical low pressure low temperature plasmas the effect of cascades is even smaller and therefore negligible. In summary, the rotational population determined via the Q branch emission can be considered as a direct image of the ground state rotational distribution.

This fact is employed in using the Q branch emission of the Fulcher-α transition as gas temperature diagnostic (see for example [13, 14, 15, 27, 28, 29]). Via optical emission spectroscopy measurements, the emissivity $\epsilon^{v',N'}$ of a rovibrational emission line originating from the level with quantum numbers v' and N' in the $d\ ^3\Pi_u^-$ state is determined. The emissivity is proportional to the population density of the level, $n^{v',N'}$, the Hönl-London factor $S^{N'}$ and the statistical weight of $(2N'+1)$ [30]:

$$\epsilon^{v',N'} \propto \frac{S^{N'}}{(2N'+1)}\, n^{v',N'}. \tag{1}$$

When a Boltzmann distribution according to the rotational temperature T_{rot} is present in the rotational levels, the population density can be parametrized as

$$\frac{n^{v',N'}}{n^{v',N'=1}} \propto g\,(2N'+1)\,exp\left(\frac{\Delta E_{rot}(N')}{k_{\mathrm{B}}\,T_{rot}}\right) \tag{2}$$

where g denotes the degeneracy arising from the nuclear spin and $\Delta E_{rot}(N')$ is the energy difference between the level N' and the lowest rotational level

$N' = 1$ [30]. Using the above two equations, the following proportionality for the emissivity is ensued:

$$\epsilon^{v',\,N'} \propto g\, S^{N'}\, exp\left(\frac{\Delta E_{rot}(N')}{k_{\mathrm{B}}\, T_{rot}}\right). \tag{3}$$

Hence, plotting $ln\left[\epsilon^{v',\,N'}/(g\, S^{N'})\right]$ against $\Delta E_{rot}(N')$ yields the rotational temperature via the slope of a linear fit. For hydrogen, the nuclear-spin degeneracy leads to an intensity alteration of the lines originating from odd or even numbered rotational levels by three to one (for deuterium, the alteration is in reverse one to two) [30]. As the magnitude of triplet splitting is very small and cannot be resolved for the Fulcher-α $^3\Pi \rightarrow {}^3\Sigma$ transition, the emission has the appearance of a singlet $^1\Pi \rightarrow {}^1\Sigma$ transition [19] and the corresponding formulas for the Hönl-London factors [30] can be used.

In order to correlate the rotational temperature $T_{rot}\left(d\ ^3\Pi_u^-, v'\right)$ determined in the excited $d\ ^3\Pi_u^-, v'$ state of the Fulcher-α transition with the one in the ground state $T_{rot}(X\ ^1\Sigma_g^+, v = 0)$, a correction with the ratio of the rotational constants B_v of the ground and excited state (which can be found in [31]) has to be carried out [16, 32]:

$$T_{gas} = T_{rot}\left(X\ ^1\Sigma_g^+, v = 0\right) = \frac{B_v\left(X\ ^1\Sigma_g^+, v = 0\right)}{B_v\left(d\ ^3\Pi_u^-, v'\right)}\, T_{rot}\left(d\ ^3\Pi_u^-, v'\right). \tag{4}$$

In the electronic ground state the rotational levels usually thermalize with the heavy particles (at least the levels with small N) which means the determined value of $T_{rot}\left(X\ ^1\Sigma_g^+, v = 0\right)$ is assumed to be equal to the gas temperature.

It should be noted, that a simplification is made during this back-projection of the rotational population from the excited to the ground electronic state: Equation (4) implicitly assumes that the population of all $d\ ^3\Pi_u^-, v'$ states solely arises from the $X\ ^1\Sigma_g^+, v = 0$ state. However, dependent on the vibrational temperature of the ground state also other vibrational states might contribute significantly. As the Franck-Condon principle holds for electron impact excitation from the $X\ ^1\Sigma_g^+$ to the $d\ ^3\Pi_u^-$ state [33], the impact of this simplification can be assessed: First, a vibrational Boltzmann distribution in the $X\ ^1\Sigma_g^+$ is calculated with a vibrational temperature T_{vib}. It is assumed that in each vibrational state the same rotational temperature (and a Boltzmann distribution) is present which is reasonable due to the long lifetime of the states what leads to a thermalization of the rotational population. The relative vibrational distribution of the ground state is then transferred into the $d\ ^3\Pi_u^-, v'$ states according to the Franck-Condon factors from [22] what reveals for each vibrational state v' the share of the population arising from the particular v state in the electronic ground state. For vibrational temperatures of several thousand Kelvin typically present in low temperature H_2 or D_2 plasmas, the $d\ ^3\Pi_u^-, v' = 2$ and 3 states are basically only populated from the $X\ ^1\Sigma_g^+, v = 0$ state whereas the $d\ ^3\Pi_u^-, v' = 1$ state also receives a small share from the $X\ ^1\Sigma_g^+, v = 1$ state. The $d\ ^3\Pi_u^-, v' = 0$ and state gets populated considerably from multiple

states in the electronic ground state: For H_2 from $v = 0, 1, 2$ and for D_2 from $v = 0, 1, 2, 3$. In summary, the simplification can be considered reasonable for the back-projection of the rotational temperatures of the $d\ ^3\Pi_u^-, v' = 2$ and 3 states and to a lesser extent also for $v' = 1$. Only for the $v' = 0$ state the simplification of equation (4) leads to an overestimation of $T_{rot}\left(X\ ^1\Sigma_g^+, v = 0\right)$ in general, although the effect is only 10% in maximum both for H_2 and D_2 for $T_{vib} < 10\ 000$ K. Therefore the simplification can be regarded legitimate for all the considered vibrational levels of the $d\ ^3\Pi_u^-$ state.

As already pointed out, the rotational levels in the electronic ground state typically follow a non-Boltzmann distribution. The shape can be described by a two-temperature population where the states with $N \lesssim 5$ follow a "cold" population according to the gas temperature whereas the "hot" rotational temperature is in the range of a few thousand K and describes levels with $N \gtrsim 7$. In low pressure low temperature discharges, the most probable process behind the hot distribution is the recombinative desorption of hydrogen occurring at the wall of the discharge vessel [9]. This process strongly depends on the surface material, its temperature and the amount of atomic hydrogen or impurity particles present on the surface (see for example [34, 35, 36, 37, 38, 39]) which makes a quantitative consideration very difficult.

Concerning the utilization of the Fulcher transition for determining the gas temperature, it is important to check which levels are described by the cold temperature and which are not. Often the first four to five rotational levels in the electronic ground state thermalize with the gas temperature (see for example [5, 6, 8, 9, 11, 12]) but this strongly depends on the value of the gas temperature: When its value decreases - for example due to active cooling of the discharge vessel - the number of levels which are in thermal equilibrium with T_{gas} also decreases due to the lower energy of the heavy particles [27, 40]. As a a-priori assessment of the number of thermalized levels is hardly possible, a consideration of non-thermalized levels in the evaluation can lead to an overestimation of the gas temperature (this will be demonstrated in sections 5.1 and 5.2). Therefore care has to be taken which levels are assigned to the cold population [32].

3. Gas temperature determination via the second positive system of nitrogen

One of the standard molecular emission bands used for determining the gas temperature of a discharge via OES is the $C\ ^3\Pi_u \rightarrow B\ ^3\Pi_g$ transition (also called the second positive system) in N_2 [16]. Due to the higher mass of nitrogen compared to hydrogen, the individual rovibrational lines of this transition cannot be resolved. The emission can only be separated into vibrational bands which are grouped together in sequences according to the difference of the upper and lower vibrational quantum number $\Delta v = v' - v''$ in a wavelength interval from 280 to 470 nm. Due to the strong overlap which makes a direct determination of the rotational population impossible, a simulation of the relative intensity of the emission band has been implemented.

The simulation calculates a vibrational population in the electronic ground state $X\ ^1\Sigma_g^+$ according to a Boltzmann distribution with a vibrational temperature T_{vib}. This population is projected into the excited $C\ ^3\Pi_u$ state according to the Franck-Condon principle (the Franck-Condon factors are taken from [41]) which implies an electron impact excitation process. In the next step, the rotational population is calculated for each vibrational level in the $C\ ^3\Pi_u$ state assuming a Boltzmann distribution with a rotational temperature T_{rot}. For determining the wavelength position of the rovibrational emission lines, the energy levels of the individual states within the electronic $C\ ^3\Pi_u$ and $B\ ^3\Pi_g$ states have to be known. There exist three sub-states each (as they are $^3\Pi$ states) and both states can be assigned to Hund's case (a) for low rotational quantum number, changing to (b) with high J. Λ-doubling can be neglected due to the small splitting of less than 10^{-4} eV [30]. The formulas for deriving the energy of the rovibrational levels are taken from [30] whereas the required coupling constants and molecular constants can be found in [42] and [43] respectively. All 27 possible branches are considered for determining the emission spectrum in the simulation. The Hönl-London factors and transition probabilities $A_{ik}^{v',v''}$ needed for calculating the relative intensity of the particular rovibrational emission line can be found in [44] and [41]. For the Gaussian profile of the particular emission lines, the full width at half maximum of the apparatus profile is used in the simulation as the Doppler width of N_2 emission is much more smaller being in the range of 1 pm for the typical heavy particle temperatures in low pressure discharges.

In general, both the vibrational temperature and the rotational temperature of the N_2 molecule can be determined from the simulation of the band system. However, for the gas temperature evaluation presented in this paper only the simulation of the $\Delta v = 0 - 2 = -2$ band located at 380 nm is considered which is one of the standard band utilized for this purpose [16]. Its simulated relative intensity is fitted to the measured one via varying the rotational temperature (see Figure 4 for an exemplary fit of simulated spectrum to a measured one). The determined value of $T_{rot}\left(C\ ^3\Pi_u, v'=0\right)$ has to be corrected according to the rotational constants for obtaining the gas temperature [16] similarly to the Fulcher transition in hydrogen:

$$T_{gas} = T_{rot}\left(X\ ^1\Sigma_g^+, v=0\right) = \frac{B_v\left(X\ ^1\Sigma_g^+, v=0\right)}{B_v\left(C\ ^3\Pi_u, v'=0\right)}\, T_{rot}\left(C\ ^3\Pi_u, v'=0\right). \quad (5)$$

The error for the determination of the gas temperature is strongly dependent on the spectral resolution of the optical system. For low resolution, the structure of the emission band smears out leading to a high error. For the present spectroscopic setup, the error can be estimated to be $\Delta T_{gas} \approx \pm 50$ K.

4. Experimental setup

The experimental setup consists of a cylindrical quartz glass discharge vessel which has a length of 40 cm and a diameter of 10 cm. The vessel is attached

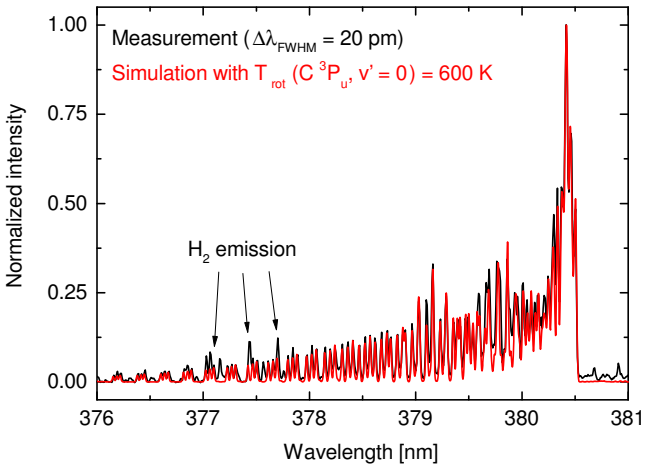

Figure 4: Exemplary measurement and fitted simulation of the relative intensity of the $\Delta v = v' - v'' = 0 - 2 = -2$ transition of the second positive system of N_2 for a 1 Pa ICP discharge operated at 600 W with a 20% admixture of nitrogen to hydrogen.

to the vacuum system at the ends of the cylinder (see Figure 5). A helical ICP antenna with five windings is utilized. It is placed in the middle of the discharge vessel with respect to the axial direction. The solenoid is connected to the RF generator which operates at a frequency of 13.56 MHz via a matching network. The investigations presented in this paper have been carried out at the maximum available RF power of 600 W unless specifically noted otherwise. The working gas is fed to the discharge vessel from the left and is pumped at the right side where the pressure is adjusted via limiting the pumping speed. The working gas pressure is measured via a capacitive pressure gauge before plasma ignition whereas the background pressure which is typically below 10^{-7} mbar is measured with a cold cathode gauge.

Optical emission spectroscopy measurements are performed with a wavelength and absolutely calibrated high-resolution spectrometer (Acton Series SP-2756i, grating with 1800 grooves/mm, Princeton Instruments PIXIS:2KB CCD camera) along an axial line of sight (radially centered, LOS depicted in Figure 5). The width of the LOS is limited by a 1 cm aperture stop placed in front of the light collecting optics. It consists of a quartz lens which collimates the plasma emission into an optical fiber placed in the focal point of the lens. The fiber guides the light towards the entrance slit of the spectrometer. The full width at half maximum of the Gaussian apparatus profile is 18 pm at a wavelength of 650 nm. Such a resolution is required for separating the individual Q lines of the Fulcher transition for hydrogen and deuterium. It should be noted that the measured line intensities represent line-of-sight averaged values, therefore also the measured rotational populations and hence the determined temperatures have to be treated as line-of-sight averaged.

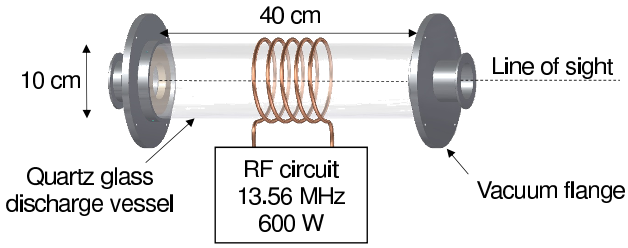

Figure 5: Sketch of the experimental setup.

5. Results and discussion

5.1. Hydrogen plasmas

In all investigated discharges the non-Boltzmann character of the rotational population is evident and very similar to the studies carried out by other groups mentioned in the introduction. Figure 6 shows exemplarily the rotational distributions of the first four vibrational levels within the $d\,^3\Pi_u^-$ state recorded at 1 Pa. In general, the first twelve lines of the Q branch have been considered for the evaluation for the $v' = 0$ & 1 states. For $v' = 2$, the states $N' > 9$ are above the dissociation limit ($H_2 \rightarrow H(1s) + H(2s)$), leading to a decreased intensity of the corresponding emission lines due to the occurring predissociation processes. The same is true for lines originating from $v' = 3$, $N' \geq 4$. States disturbed by predissociation (depicted with open symbols in Figure 6) and lines which are strongly overlapped by neighboring emission (like the one from $v' = 1$ & $N' = 10$) have been omitted in the evaluation.

As demonstrated in Figure 6 for $v' = 0$, the rotational distribution in the individual vibrational states can be fitted very well by assuming a two-temperature distribution for the rotational population according to

$$n^{N'} = \tilde{n}^{N'}\left(T_{rot,\,1}\right) + \beta\,\hat{n}^{N'}\left(T_{rot,\,2}\right) \tag{6}$$

where $n^{N'}$ denotes the relative population in the state with rotational quantum number N'. $\tilde{n}^{N'}\left(T_{rot,\,1}\right)$ and $\hat{n}^{N'}\left(T_{rot,\,2}\right)$ are Boltzmann populations according to a cold temperature $T_{rot,\,1}$ and a hot temperature $T_{rot,\,2}$ respectively. The parameter β is a weighting factor. The two-temperature characteristics is also present in the $v' = 3$ state, but a fit cannot be carried out due to the influence of predissociation on higher lying N states.

The determination of the hot temperature via a fitting routine is sometimes difficult as the emission lines from the high rotational states are rather weak and overlapped, especially when nitrogen emission is present. The most reliable fit of $T_{rot,\,2}$ is obtained in the $v' = 0$ state as the corresponding emission lines are stronger compared to those from the higher vibrational levels. Therefore, the hot temperature is only fitted in this state and $T_{rot,\,2}$ of the $v' = 1$ and 2 states is calculated by the following approach: First, $T_{rot,\,2}\left(d\,^3\Pi_u^-, v' = 0\right)$ is projected into the $v = 0$ state in the electronic ground state according to the

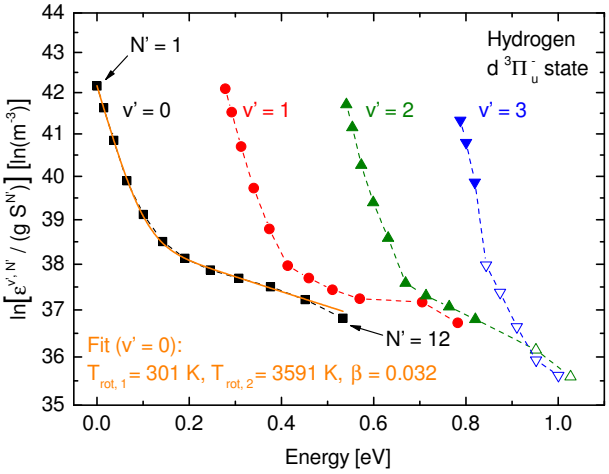

Figure 6: Rotational distributions of the first four vibrational states in the upper state of the Fulcher-α transition obtained for 1 Pa of H_2. For $v' = 0$ a fit according to a two-temperature distribution is also shown. The energy levels of the particular rovibrational states have been taken from [24, 22] (the energy of high N-levels has been determined via a quadratic extrapolation from [24]). Those levels suffering from a reduced population density caused by predissociation are depicted in open symbols.

rotational constants. Second, $T_{rot,\,2}\left(X\ ^1\Sigma_g^+, v' = 0\right)$ is projected again upwards into the $d\ ^3\Pi_u^-, v' = 1$ and 2 states. This approach is reasonable as it relies on the same simplification as described for equation (4) in section 2. Hence, the fitting routine of the rotational population in the $d\ ^3\Pi_u^-, v' = 1$ and 2 states has only the cold temperature and the weighting factor as free parameter.

Table 1 summarizes the fitting parameters obtained for the 1 Pa hydrogen plasma (it also contains the fitting parameters for the nitrogen/hydrogen mixtures but they are discussed later). The cold rotational temperatures decrease with increasing vibrational quantum number which has also been observed in other studies [32]. As the relative rotational distribution is preserved during the electron impact excitation process (see section 2), the fitted temperature should only depend on the energy difference of the rotational states. As this energy difference decreases for higher v levels due to the decreasing rotational constants, also the rotational temperature decreases. When this effect is considered, an agreement of the cold rotational temperatures within the error bar is obtained. The same effect also leads to the decreasing behavior of the derived hot rotational temperatures.

The weighting factor of the hot population coincides within the error bar for $v' = 1$ and 2 whereas β is larger for $v = 0$. This can be explained as the population of the $d\ ^3\Pi_u^-, v' = 0$ state - in contrast to the $v' = 1$ and 2 states - originates from multiple vibrational levels in the $X\ ^1\Sigma_g^+$ state (see section 2). As β seems to increase for higher vibrational states in the electronic ground

Table 1: $T_{rot,\,1}$, β, and $T_{rot,\,2}$ of the individual vibrational levels in the $d\ ^3\Pi_u^-, v' = 0$ state determined from the Fulcher-α transition for a variation of the nitrogen admixture to hydrogen. The given errors reflect the ones obtained from the fitting procedure. As $T_{rot,\,2}(v' = 1, 2\ \&\ 3)$ is calculated from $T_{rot,\,2}(v' = 0)$ (see section 2), no error is given there.

N_2 admixture to H_2 [%]	v'	$T_{rot,\,1}$ [K]	β	$T_{rot,\,2}$ [K]
0	0	301 ± 4	0.032 ± 0.001	3591 ± 122
	1	284 ± 5	0.022 ± 0.001	3403
	2	267 ± 8	0.022 ± 0.001	3216
20	0	323 ± 7	0.038 ± 0.002	3225 ± 142
	1	300 ± 8	0.028 ± 0.001	3056
	2	286 ± 18	0.026 ± 0.003	2888
50	0	337 ± 17	0.042 ± 0.016	3245 ± 1463
	1	309 ± 30	0.040 ± 0.007	3076
	2	303 ± 20	-	2906

state (see for example Figure 3 in reference [9] or Figure 4 in reference [45]), a contribution of states besides the $v = 0$ state leads to an increased value of the weighting factor in the excited state. However, a quantitative assessment of this effect cannot be carried out as the ground state rovibrational distribution is not accessible with the present experimental setup. It should be noted that a varying β in the ground state only influences the β determined for the $d\ ^3\Pi_u^-, v' = 0$ state, but not the rotational temperatures which can be considered equal for all vibrational levels in the $X\ ^1\Sigma_g^+$ state (see again references [9, 45]).

Figure 7 shows the rotational distribution of the $v = 0$ state in the electronic ground state of hydrogen normalized to the level $N = 1$. It has been determined from projecting the rotational distributions of the $d\ ^3\Pi_u^-, v' = 1$ and 2 states into the ground state and averaging the obtained relative population densities. The shape of the obtained distribution is very similar to the ones obtained from rotational-state resolved recombinative desorption measurements of atomic hydrogen (see for example [46, 47]) which encourages the hypothesis that the hot rotational population arises from this process. Although the weighting factor of the hot population is only 0.022, it leads to an overpopulation of more than 5 orders of magnitude for levels with high rotational quantum number compared to a pure Boltzmann distribution according to $T_{rot,\,1}$. This demonstrates the necessity of considering the correct rotational population for calculating molecular reaction rates in low pressure hydrogen discharges.

In order to check if the cold rotational temperature coincides with the gas temperature, measurements have been performed for discharges operated at 1 Pa pressure with varying nitrogen admixture to hydrogen. From the emission of the second positive system of N_2 T_{gas} can be obtained as described in section 3. Table 1 summarizes the obtained fitting parameters of the rotational distributions in the $d\ ^3\Pi_u^-$ state. With increasing N_2 admixture, the evaluation of the Fulcher-α spectrum gets more difficult due to the strong overlap with the emission of the first positive system of nitrogen ($B\ ^3\Pi_g \rightarrow A\ ^3\Sigma_u^+$ transition). This results in increasing fitting errors and above a nitrogen content of 50% the

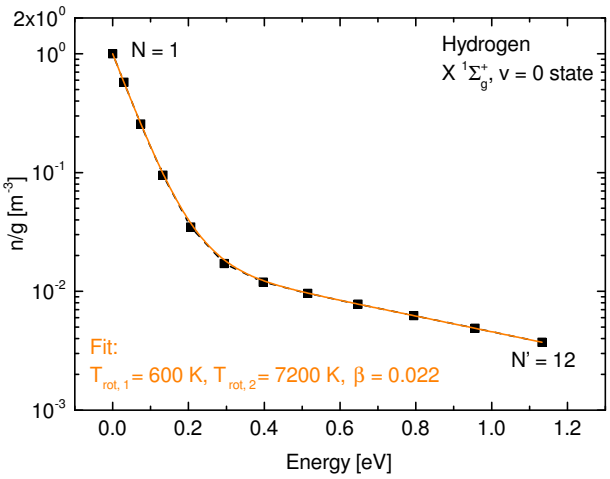

Figure 7: Relative rotational population in the $X\ ^1\Sigma_g^+, v = 0$ state of hydrogen determined from projecting the rotational distributions of the $d\ ^3\Pi_u^-, v' = 1$ and 2 states shown in Figure 6 to the ground state and averaging them. The obtained parameters are: $T_{rot,\,1} = 600$ K, $\beta = 0.022$ and $T_{rot,\,2} = 7\ 200$ K.

evaluation could not be carried out at all.

Within the vibrational levels, the rotational temperatures and the weighting factors follow the same trends for all nitrogen admixtures as described for pure hydrogen plasmas. For increasing N_2 content, an increase in $T_{rot,\,1}$ and β is observed whereas $T_{rot,\,2}$ decreases. An explanation of the behavior of the hot rotational temperature and the weighting factor requires the detailed consideration of the recombinative desorption process of atomic hydrogen. Unfortunately this cannot be carried out as on the one hand side the required data is not available in the literature. On the other hand side, also the exact conditions of the surface as the coverage with atomic hydrogen, the roughness of the surface, etc. are not know for the present experimental setup. However, the rising weighting factor points towards an increased importance of recombinative desorption with higher nitrogen content.

As the cold rotational temperature in the $d\ ^3\Pi_u^-$ state is determined by the gas temperature, a projection of $T_{rot,\,1}$ into the ground state has been carried out. Figure 8 shows $T_{rot,\,1}\left(X\ ^1, v = 0\right)$ calculated from the $d\ ^3, v' = 0, 1, 2$ states together with T_{gas} evaluated from the second positive system of nitrogen. In general, a very good agreement concerning the rotational temperatures of hydrogen and nitrogen is obtained underlining the possibility of determining T_{gas} via the Fulcher-α transition. As already indicated from the increasing values of $T_{rot,\,1}$ summarized in Table 1, T_{gas} increases with rising nitrogen content.

It can be seen from Figure 6 that only the first four rotational levels follow a linear trend and can therefore be described as thermalized with $T_{rot,\,1}$.

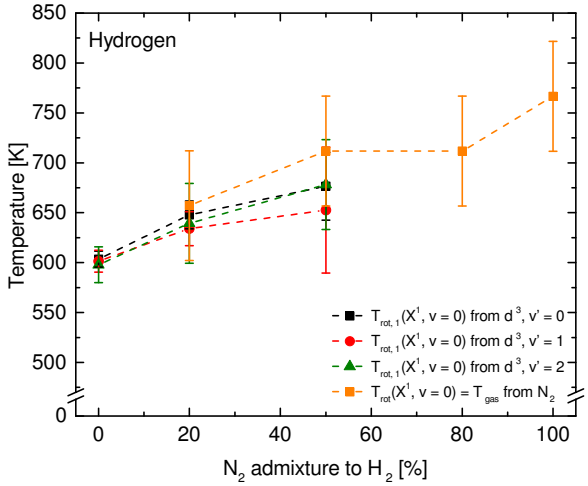

Figure 8: Rotational temperatures of the electronic ground state of H_2 and N_2 for a variation of the nitrogen admixture to hydrogen. For the Fulcher-α system of H_2, the temperatures determined from the first three vibrational levels in the excited state are plotted.

The fifth level, which is often also included in a linear fit for determining the gas temperature [32, 29] already deviates slightly from linearity what leads to an overestimation of T_{gas}. The magnitude of this overestimation is strongly dependent on the relevance of the hot population which is described by the weighting factor. Table 2 shows a comparison of the cold rotational temperature obtained from the two-temperature fit with T_{gas} derived from a linear fit considering the first five rotational levels for the 1 Pa hydrogen discharge. For the two-temperature fit, the fitting errors are rather small and a good agreement between the individual vibrational states is achieved. The averaged gas temperature is 601 ± 12 K. In contrast, a span of 50 K lies between the highest and lowest gas temperature values determined with the linear fit and the fitting errors are much larger. Averaging over the obtained temperatures yields 737 ± 45 K and hence a much higher value compared to the two-temperature fit. One should therefore not restrict the measurements to the first five Q lines in general as slight deviations from linearity might not be obvious but they could lead to a large overestimation of the gas temperature.

5.2. Deuterium plasmas

For deuterium, the two-temperature distribution of the rotational population is also present in the investigated discharges. Figure 9 shows the distribution for the first four vibrational levels in a 1 Pa deuterium plasma together with a two-temperature fit for $v' = 0$. For the evaluations, the first 13 rotational levels have been considered, only for $v' = 2$ the line positions available in literature are restricted to the first eight levels. Strongly overlapped lines or lines where

Table 2: T_{gas} determined from the two-temperature fit and from a linear fit considering the first five rotational levels within the vibrational states $v' = 0$, 1 and 2 of the Fulcher-α transition for a 1 Pa hydrogen plasma.

v'	T_{gas} [K], two-temperature fit	T_{gas} [K], linear fit
0	603 ± 9	759 ± 47
1	602 ± 10	706 ± 34
2	598 ± 17	747 ± 53

not data is present in literature are omitted. As the rovibrational levels have a smaller energy difference in comparison to hydrogen, predissociation is not relevant for the considered levels.

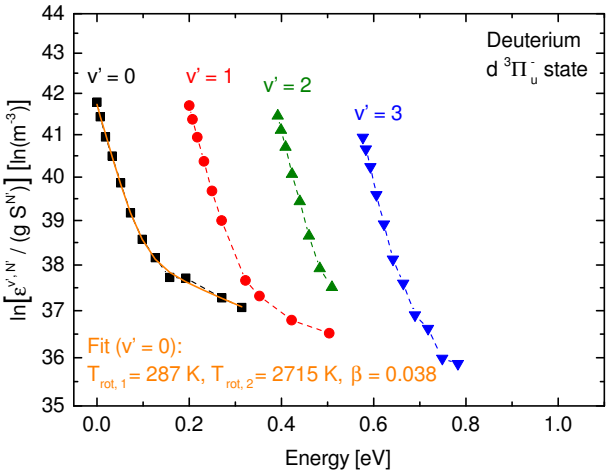

Figure 9: Rotational distributions of the first four vibrational states in the upper state of the Fulcher-α transition obtained for 1 Pa of D_2. For $v' = 0$ a fit according to a two-temperature distribution is also shown. The energy levels of the particular rovibrational states have been taken from [48, 22] (the energy of high N-levels has been determined via a quadratic extrapolation from [48]).

The fitting parameters obtained for varying nitrogen admixture to deuterium are summarized in Table 3. In general the scatter of the measured rotational distributions is higher as in hydrogen. This arises from the fact that the single ro-vibrational emission lines are grouped more closely together what results in a larger overlap of the individual lines for deuterium. For a nitrogen content of 50%, the rotational populations of the $v' = 2$ and 3 states could not be determined any more due to strong overlap with nitrogen emission. Similar to hydrogen, the rotational temperatures show a decrease with increasing vibrational quantum number what can be attributed to the changing rotational constants. The obtained values of β are the same within the error bars for the states $v' = 1, 2$ and 3. Only the weighting factor in the $v' = 0$ level is higher

as in hydrogen due to its population from multiple vibrational states in the electronic ground state. The ground state rotational population for the pure deuterium discharge is shown in Figure 10. It has been determined from the averaged rotational distributions of the $d\ ^3\Pi_u^-, v' = 1, 2$ and 3 states and as with hydrogen, its shape is very similar to the ones obtained from rotational-state resolved recombinative desorption measurements [37, 39].

Table 3: $T_{rot,\ 1}$, β, and $T_{rot,\ 2}$ determined from the Fulcher-α transition for a variation of the nitrogen admixture to deuterium. The given errors reflect the ones obtained from the fitting procedure. As $T_{rot,\ 2}(v' = 1, 2\ \&\ 3)$ is calculated from $T_{rot,\ 2}(v' = 0)$ (see section 2), no error is given there.

N_2 admixture to D_2 [%]	v'	$T_{rot,\ 1}$ [K]	β	$T_{rot,\ 2}$ [K]
0	0	287 ± 10	0.038 ± 0.005	2715 ± 324
	1	276 ± 4	0.022 ± 0.001	2615
	2	258 ± 5	0.021 ± 0.003	2514
	3	248 ± 7	0.024 ± 0.002	2414
20	0	292 ± 21	0.047 ± 0.021	2249 ± 1108
	1	277 ± 11	0.030 ± 0.002	2166
	2	266 ± 17	0.032 ± 0.008	2083
	3	258 ± 26	0.034 ± 0.010	2000
50	0	317 ± 78	0.058 ± 0.029	1965 ± 723
	1	322 ± 48	-	1890
	2	-	-	1774
	3	-	-	1703

For varying nitrogen content, the rotational temperatures and the weighting factors show the same dependency as observed in hydrogen. Furthermore, the absolute values of $T_{rot,\ 1}$ and β are comparable to those obtained for H_2. Only the hot rotational temperature is considerably smaller in deuterium indicating an isotope-dependency of the recombinative desorption process which has also been observed in general in [37, 39].

The cold rotational temperatures projected into the electronic ground state are given in Figure 11 together with the gas temperature obtained from the second positive system of nitrogen. The values obtained from the Fulcher-α emission of D_2 are always below T_{gas} from N_2 although the corresponding error bars still overlap. As no difference is detectable between hydrogen and deuterium concerning the gas temperature evaluated from the N_2 emission, it can be assumed that in contrast to hydrogen the cold rotational temperature determined from the Fulcher-α emission of deuterium underestimates T_{gas} slightly. However, a definite statement is difficult as no independent measurement of the gas temperature is present in the pure deuterium discharge and the error bars of the cold rotational temperatures are rather large with nitrogen admixture.

Concerning the comparison of the gas temperature obtained from the two-temperature fit and the one from a linear fit of the first five rotational levels, the results are summarized in Table 4. For the two-temperature fit, the agreement of the individual temperatures is very good whereas for the linear fit a span of

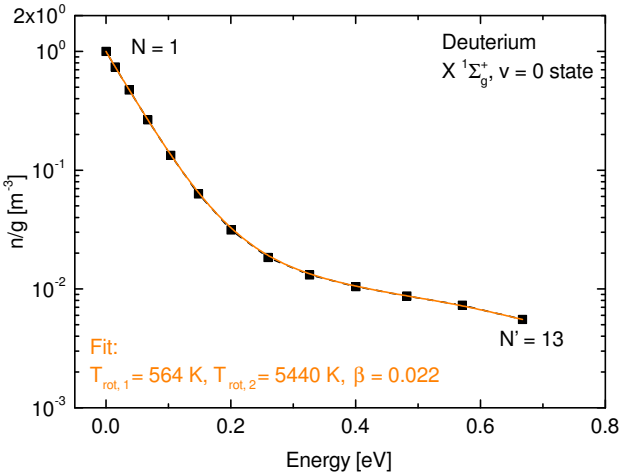

Figure 10: Relative rotational population in the $X\ ^1\Sigma_g^+, v = 0$ state of deuterium determined from projecting the rotational distributions of the $d\ ^3\Pi_u^-, v' = 1, 2$ and 3 states shown in Figure 9 to the ground state and averaging them. The obtained parameters are: $T_{rot,\ 1} = 564$ K, $\beta = 0.022$ and $T_{rot,\ 2} = 5\ 440$ K.

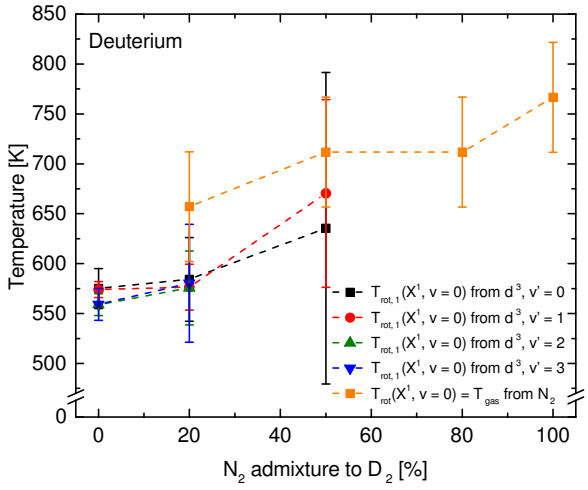

Figure 11: Rotational temperatures of the electronic ground state of D_2 and N_2 respectively for a variation of the nitrogen admixture to hydrogen. For the Fulcher-α system of D_2, the temperatures determined from the first four vibrational levels in the excited state are plotted.

about 50 K is present. The overestimation by the linear fit is smaller compared to hydrogen, an average gas temperature of 600 ± 18 K is obtained whereas the one of the two-temperature fit is 568 ± 14 K.

Table 4: T_{gas} determined from the two-temperature fit and from a linear fit considering the first five rotational levels of the Fulcher-α transition for a 1 Pa deuterium plasma.

v'	T_{gas} [K], two-temperature fit	T_{gas} [K], linear fit
0	575 ± 20	631 ± 30
1	578 ± 8	593 ± 9
2	559 ± 12	591 ± 15
3	559 ± 16	586 ± 11

6. Summary

It is well known that typically a non-Boltzmann rotational distribution is present in the electronic ground state of the hydrogen molecule but direct measurements are complicated and expensive. Via the molecular Fulcher-α transition, an indirect determination of the relative ground state rotational population has been demonstrated both for hydrogen and deuterium. The obtained rotational populations can be described by a two-temperature distribution where the cold part is thermalized with the gas temperature and the hot part most likely arises from recombinative desorption of hydrogen from the discharge vessel wall. In general, no substantial difference between the rotational distributions for H_2 and D_2 has been found, only the hot rotational temperature is smaller in deuterium what points towards an isotope-dependency of the recombinative desorption process. The hot distribution is usually neglected when determining the gas temperature of a plasma from the Fulcher-α emission. This simplification can lead to a strong overestimation of the obtained value of T_{gas} especially for hydrogen, whereas the effect is less pronounced for deuterium. Concluding, the Fulcher-α transition provides the possibility of an easy but sensitive measurement of the relative rotational population in the $X\ ^1\Sigma_g^+, v = 0$ state up to high rotational quantum numbers. An assessment of this population is highly relevant as the rotational excitation in the electronic ground state can have a considerable impact on molecular reaction rates in low pressure plasmas in addition to the widely acknowledged influence of vibrational excitation.

Acknowledgments

The authors would like to thank the Deutsche Forschungsgemeinschaft (DFG) for their support within the project BR 4904/1-1.

This work has been carried out within the framework of the EUROfusion Consortium and has received funding from the Euratom research and training programme 2014-2018 under grant agreement No 633053. The views and opinions expressed herein do not necessarily reflect those of the European Commission.

References

[1] Capitelli M and Gorse C 2005 *IEEE Trans. Plasma Sci.* **33** 1832–1844

[2] Celiberto R, Janev R K, Laricchiuta A, Capitelli M, Wadehra J M and Atems D E 2001 *At. Data. Nucl. Data Tables* **77** 161 – 213

[3] Wadehra J M 1984 *Phys. Rev. A* **29** 106–110

[4] Bonnie J H M, Eenshuistra P J and Hopman H J 1988 *Phys. Rev. A* **37** 1121–1132

[5] Stutzin G, Young A, Schlachter A, Leung K and Kunkel W 1989 *Chem. Phys. Lett.* **155** 475 – 480

[6] Stutzin G C, Young A T, Döbele H F, Schlachter A S, Leung K N and Kunkel W B 1990 *Rev. Sci. Instrum.* **61** 619–621

[7] Meulenbroeks R F G, Engeln R A H, van der Mullen J A M and Schram D C 1996 *Phys. Rev. E* **53** 5207–5217

[8] Mosbach T, Katsch H M and Döbele H F 2000 *Phys. Rev. Lett.* **85** 3420–3423

[9] Vankan P, Schram D and Engeln R 2004 *Chem. Phys. Lett.* **400** 196 – 200

[10] Péalat M, Taran J E, Bacal M and Hillion F 1985 *J. Chem. Phys.* **82** 4943–4953

[11] Wagner D, Dikmen B and Döbele H F 1998 *Plasma Sources Sci. Technol.* **7** 462–470

[12] Gabriel O, van den Dungen J J A, Schram D C and Engeln R 2010 *J. Chem. Phys.* **132** 104305

[13] Lavrov B P, Ostrovskii V N and Ustimov V I 1979 *Opt. Spectrosc. (USSR)* **47** 30 – 34

[14] Lavrov B P 1980 *Opt. Spectrosc. (USSR)* **48** 375 – 380

[15] Lavrov B P and Tyutchev M V 1984 *Acta Physica Hungarica* **55** 411 – 426

[16] Bruggeman P J, Sadeghi N, Schram D C and Linss V 2014 *Plasma Sources Sci. Technol.* **23** 023001

[17] Farley D R, Stotler D P, Lundberg D P and Cohen S A 2011 *J. Quant. Spectrosc. Radiat. Transfer* **112** 800 – 819

[18] Dieke G H 1935 *Phys. Rev.* **48** 610–614

[19] Dieke G H and Blue R W 1935 *Phys. Rev.* **47** 261–272

[20] Kovacs I, Lavrov B P, Tyutchev M V and Ustimov V I 1983 *Opt. Spectrosc. (USSR)* **54** 537 – 538

[21] Sharp T E 1971 *Atom. Data Nucl. Data Tables* **2** 119 – 169

[22] Fantz U and Wünderlich D 2006 *Atom. Data. Nucl. Data Tables* **92** 853 – 973 full data set available as IAEA INDC(NDS)-457 report

[23] Yamasaki D, Kado S, Xiao B, Iida Y, Kajita S and Tanaka S 2006 *J. Phys. Soc. Jpn.* **75** 044501

[24] Dieke G H 1972 *The hydrogen molecule wavelength tables of Gerhard Heinrich Dieke* (Wiley-Interscience) edited by Crosswhite H M

[25] Freund R S, Schiavone J A and Crosswhite H M 1985 *J. Phys. Chem. Ref. Data* **14** 235–383

[26] Astashkevich S A and Lavrov B P 2002 *Opt. Spectrosc.* **92** 818–850

[27] Sobolev N N (ed) 1989 *Electron-excited Molecules in Nonequilibrium Plasma* (*Proceedings of the Lebedev Physics Institute, Academy of Sciences of the USSR* vol 179) (Nova Science Publishers)

[28] Tomasini L, Rousseau A, Gousset G and Leprince P 1996 *J. Phys. D: Appl. Phys.* **29** 1006–1013

[29] Fantz U 2004 *Contrib. Plasma Physics* **44** 508–515

[30] Herzberg G 1950 *Molecular spectra and molecular structure, I. Spectra of diatomic molecules* vol 2 (D. van Nostrand Company, Inc)

[31] Huber K P and Herzberg G (data prepared by Gallagher J W and Johnson R D III) "Constants of Diatomic Molecules" in *NIST Chemistry WebBook, NIST Standard Reference Database Number 69*, Eds. Linstrom P J and Mallard W G, National Institute of Standards and Technology, Gaithersburg MD, 20899, http://webbook.nist.gov, (retrieved May 20, 2016)

[32] Astashkevich S A, Käning M, Käning E, Kokina N V, Lavrov B P, Ohl A and Röpcke J 1996 *J. Quant. Spectrosc. Radiat. Transfer* **56** 725 – 751

[33] Villarejo D, Stockbauer R and Inghram M G 1969 *J. Chem. Phys.* **50** 1754–1762

[34] Rutigliano M, Gamallo P, Sayós R, Orlandini S and Cacciatore M 2014 *Plasma Sources Sci. Technol.* **23** 045016

[35] Zacharias H 1988 *Appl. Phys. A* **47** 37–54

[36] Schröter L, David R and Zacharias H 1991 *Surface Science* **258** 259 – 268

[37] Rettner C T, Michelsen H A and Auerbach D J 1993 *J. Vac. Sci. Technol. A* **11** 1901–1906

[38] Rettner C T, Michelsen H A and Auerbach D J 1995 *J. Chem. Phys.* **102** 4625–4641

[39] Gleispach D and Winkler A 2003 *Surface Science* **537** L435 – L441

[40] Otobraev D K, Ochkin V N, Savinov S Y, Sobolev N N and Tskhai S N 1978 *JETP Lett.* **6** 392–396

[41] Gilmore F R, Laher R R and Espy P J 1992 *J. Phys. Chem. Ref. Data* **21** 1005–1107

[42] Budó A 1935 *Zeitschrift für Physik* **96** 219–229

[43] Laher R R and Gilmore F R 1991 *J. Phys. Chem. Ref. Data* **20** 685–712

[44] Kovács I 1969 *Rotational Structure in the Spectra of Diatomic Molecules* (Adam Hilger LTD, London)

[45] Gabriel O, Schram D C and Engeln R 2008 *Phys. Rev. E* **78** 016407

[46] Kolasinski K W, Shane S F and Zare R N 1991 *J. Chem. Phys.* **95** 5482–5485

[47] Shane S F, Kolasinski K W and Zare R N 1992 *J. Chem. Phys.* **97** 1520–1530

[48] Lavrov B P and Umrikhin I S 2008 *arXiv* arXiv:physics/0703114v3 [physics.optics]